European Radiology (2024) 34:155–164
https://doi.org/10.1007/s00330-023-10025-3

European Radiology
EUROPEAN SOCIETY OF RADIOLOGY

BREAST

Breast MRI in patients with implantable loop recorder: initial experience

Noam Nissan[1] · Rosa Elena Ochoa-Albiztegui[1] · Hila Fruchtman[1] · Jill Gluskin[1] · Sarah Eskreis-Winkler[1] · Joao V. Horvat[1] · Ioanna Kosmidou[2] · Alicia Meng[1] · Katja Pinker[1] · Maxine S. Jochelson[1]

Received: 17 January 2023 / Revised: 10 May 2023 / Accepted: 13 June 2023 / Published online: 9 August 2023

Abstract

Objectives To investigate the feasibility of breast MRI exams and guided biopsies in patients with an implantable loop recorder (ILR) as well as the impact ILRs may have on image interpretation.

Materials and methods This retrospective study examined breast MRIs of patients with ILR, from April 2008 to September 2022. Radiological reports and electronic medical records were reviewed for demographic characteristics, safety concerns, and imaging findings. MR images were analyzed and compared statistically for artifact quantification on the various pulse sequences.

Results Overall, 40/82,778 (0.049%) MRIs during the study period included ILR. All MRIs were completed without early termination. No patient-related or device-related adverse events occurred. ILRs were most commonly located in the left lower-inner quadrant (64.6%). The main artifact was a signal intensity (SI) void in a dipole formation in the ILR bed with or without areas of peripheral high SI. Artifacts appeared greatest in the cranio-caudal axis ($p < 0.001$), followed by the anterior–posterior axis ($p < 0.001$), and then the right–left axis. High peripheral rim-like SI artifacts appeared on the post-contrast and subtracted T1-weighted images, mimicking suspicious enhancement. Artifacts were most prominent on diffusion-weighted ($p < 0.001$), followed by T2-weighted and T1-weighted images. In eight patients, suspicious findings were found on MRI, resulting in four additional malignant lesions. Of six patients with left breast cancer, the tumor was completely visible in five cases and partially obscured in one.

Conclusion Breast MRI is feasible and safe among patients with ILR and may provide a significant diagnostic value, albeit with localized, characteristic artifacts.

Clinical relevance statement Indicated breast MRI exams and guided biopsies can be safely performed in patients with implantable loop recorder. Nevertheless, radiologists should be aware of associated limitations including limited assessment of the inner left breast and pseudo-enhancement artifacts.

Key Points

- *Breast MRI in patients with an implantable loop recorder is an infrequent, feasible, and safe procedure.*
- *Despite limited breast visualization of the implantable loop recorder bed and characteristic artifacts, MRI depicted additional lesions in 8/40 (20%) of cases, half of which were malignant.*
- *Breast MRI in patients with an implantable loop recorder should be performed when indicated, taking into consideration typical associated artifacts.*

Keywords Magnetic resonance imaging · Artifacts · Breast neoplasms

Abbreviations

AP	Anterior-posterior
CC	Cranio-caudal
DCE	Dynamic contrast-enhanced
DWI	Diffusion-weighted imaging
ECG	Electrocardiogram
EPI	Echo planar imaging
ILR	Implantable loop recorder
IQR	Interquartile range
MLO	Medio-lateral oblique
MUSE	Multiplexed sensitivity-encoding
RL	Right–left
SD	Standard deviation
SI	Signal intensity

✉ Maxine S. Jochelson
jochelsm@mskcc.org

[1] Department of Radiology, Memorial Sloan Kettering Cancer Center, New York, NY 10065, USA

[2] Department of Medicine, Memorial Sloan Kettering Cancer Center, New York, NY 10065, USA

Introduction

An implantable loop recorder (ILR) is a diagnostic monitoring device that continuously records cardiac electrical activity in order to diagnose an underlying arrhythmia or conduction system disease [1]. ILRs are discreet devices, usually inserted subcutaneously in the left prepectoral and parasternal position under local anesthesia. Equipped with a battery life of about 3 to 5 years, an ILR is an important diagnostic tool in patients with cryptogenic stroke, palpitations, and syncope [2].

In recent years, as indications for ILR placement have expanded [3], the imaging manifestations of ILR have begun to draw interest. Studies on the mammographic appearance of various brands of ILR [4–6] suggest that mammography can be safely performed among patients with ILRs, albeit with suboptimal imaging quality, increased discomfort, and increased anxiety during positioning [7].

Despite the associated technical challenges, the drive to apply MRI in the vicinity of embedded metallic hardware keeps increasing [8]. Currently available ILRs are labeled as MRI-conditional to reflect their MRI safety category [9], for both 1.5 T and 3.0 T field strengths [10]. Both cardiac and thoracic MRI studies have demonstrated that MRI scans of ILR patients can be safely executed with no impact on device function, battery life, or patient-reported symptoms [9]. While there are no absolute or relative contraindications for MRI scanning among patients with ILR, the examination of conditional ILRs should be performed within labeled scanning prerequisites specific to each device manufacturer [7]. Additional concerns have arisen regarding metal-induced susceptibility artifacts that can degrade image quality [11–13], as well as signal artifacts affecting the recorded ECG activity, which may be mistakenly interpreted as tachyarrhythmia [14, 15].

To the best of our knowledge, the impact of ILR on breast MRI examinations and procedures has yet to be reported. Therefore, the purpose of this study was to investigate our institutional experience in conducting breast MRI in this unique population, aiming to evaluate safety, image quality, and clinical considerations.

Materials and methods

Study population

This single-institution study and retrospective data analysis was approved by the Institutional Review Board and conducted in compliance with the Health Insurance Portability and Accountability Act. Using proprietary software, a computational search of our institutional radiological information system was performed; all breast MRI examinations between April 2008 and September 2022 were surveyed to identify reports containing the filter words "loop recorder." Subsequent case-by-case verification was performed to exclude misclassified cases.

MRI examination

MRI scans performed in our institution were executed on either 1.5- or 3.0-T units with a dedicated breast coil (Signa; General Electric) using a state-of-the-art MRI protocol, including fat-suppressed T2-weighted, non-fat-suppressed T1-weighted, and fat-suppressed T1-weighted dynamic contrast-enhanced (DCE) sequences before and after intravenous administration of a gadolinium-based contrast agent, with automatically generated subtraction and 3D reconstruction images. Diffusion-weighted imaging (DWI) was intermittently acquired. The complete MRI protocol is provided in Supplementary Table 1, as previously described [16]. In addition, relevant cases performed at outside facilities and submitted for second opinion review were also included; those scans included DCE sequences but varied in the MRI protocols.

Data assessment

Radiological reports and electronic medical records were reviewed for patients' demographic characteristics and clinical findings, which were categorized according to the original interpretation by one of our 32 breast radiologists. Electronic medical records were reviewed for identification of any patient- or device-related safety concerns associated with the MRI scan (i.e., any documentation of incidence related to the MRI scan). MR images were analyzed by a single fellowship-trained breast radiologist, N.N., with 12 years of experience in breast MRI.

Statistical analysis

Statistical analysis included calculation of means and standard deviations (SDs) of the acquired parameters (GraphPad Prism 5.03). The Mann–Whitney *U* test was used to evaluate the intra-individual changes between the artifacts' measurements in each axis, as well as between the various MRI sequences and between scans performed on 1.5 T vs. 3.0 T (R: A language and environment for statistical computing, 2020). Statistical significance was defined as $p < 0.05$.

Results

Patient characteristics

Overall, the term "loop recorder" appeared in 40 of 82,778 breast MRI reports, accounting for 0.049% of the cases in the study timespan. The first MRI in a patient

with loop recorder was performed in 2015, followed by a second scan in 2016 and a third in 2017. Since 2018, up to seven new patients with loop recorders underwent breast MRI, each year. The study cohort was composed of 31 patients (one with four MRIs, six with two MRIs), including 30 females and one male, with an average age of 63.6 ± 10.5 years (range: 39–85).

MRI indications for the 40 examinations among 31 patients were as follows: assessment of newly diagnosed breast cancer ($n = 16$, ten right-sided and six left-sided), high-risk surveillance ($n = 18$, including five patients with a personal history of breast cancer, four with a family history, two with high-risk lesions, and one BRCA mutation carrier), suspicious findings on other modalities ($n = 4$), and monitoring response to chemotherapy ($n = 2$). Summary of the patients' characteristics is provided in Table 1.

Safety

A case-by-case overview of the electronic medical records of all 31 patients, conducted with a mean follow-up duration of 9.2 ± 13.8 months (range: 1–48), confirmed that all examinations were finalized without early termination and no patient-related or device-related adverse events were documented.

Artifact profiles

The loop recorder and the associated artifact epicenter were most commonly localized in the left lower-inner quadrant (20/31 cases, 64.6%), whereas in the remaining 11/31 (35.4%) cases, the device was implemented in the left upper inner quadrant.

Table 1 Patient and imaging characteristics. List of patients and imaging workup characteristics. Four patients had multiple examinations and all but one had prior mammography and US available. *Patient has multiple MRIs. *PH*, personal history of breast cancer; *FH*, family history of breast cancer; *ALH*, atypical lobular hyperplasia; *CEM*, contrast-enhanced mammography

Patient	Age	Risk factors	MRI indication	Prior mammogram	Prior US
1*	74	PH, FH	High-risk screening	Yes	Yes
2	73		Pretreatment evaluation of new ca	Yes	Yes
3	85		Pretreatment evaluation of new ca	Yes	Yes
4	74	PH	High-risk screening	Yes	Yes
5*	53		Evaluating FDG uptake on PET/CT	Yes	Yes
6	53		Pretreatment evaluation of new ca	Yes	Yes
7	70		Pretreatment evaluation of new ca	Yes	Yes
8*	62	LCIS	High-risk screening	Yes	Yes
9	56	FH	High-risk screening	Yes	Yes
10	66	BRCA 2	High-risk screening	Yes	Yes
11*	67	FH	Pretreatment evaluation and post NAC response	Yes	Yes
12*	49		Evaluating response to NAC	Yes	Yes
13	69		Pretreatment evaluation of new ca	Yes	Yes
14	77		Pretreatment evaluation of new ca	Yes	Yes
15	72		Pretreatment evaluation of new ca	Yes	Yes
16*	69		High-risk screening	Yes	Yes
17	49		Pretreatment evaluation of new ca	Yes	Yes
18	73		Evaluating FDG uptake on PET/CT	Yes	Yes
19*	59	ALH	High-risk screening	Yes	Yes
20	49		Pretreatment evaluation of new ca	Yes	Yes
22	62	FH	High-risk screening	Yes	Yes
23	61		Pretreatment evaluation of new ca	Yes	Yes
24	63		High-risk screening	-	-
25	81		Pretreatment evaluation of new ca	Yes	Yes
26	65		Pretreatment evaluation of new ca	Yes	Yes
27	61	PH	Pretreatment evaluation of new ca	Yes	Yes
28	59	PH	Evaluating nipple discharge	Yes	Yes
29	66	PH	High-risk screening	Yes	Yes
30	39	FH	Evaluating enhancement on CEM	Yes	Yes
30	50		Pretreatment evaluation of new ca	Yes	Yes
31	66		Pretreatment evaluation of new ca	Yes	Yes

The main artifact due to the ILRs was a signal void in the ILR bed with or without areas of peripheral high signal intensity (SI). Altogether, ILR-induced artifacts varied among patients, axes, and sequences. A representative case illustrating the variable appearance of ILR-induced artifacts in the various MRI sequences is presented in Fig. 1.

On post-contrast T1-weighted images, signal voids were largest in the cranio-caudal axis ($p < 0.001$), measuring 6.4 ± 1.2 cm (range: 4.1–9.1) on average, followed by the anterior–posterior axis ($p < 0.001$) measuring 5.0 ± 0.9 (range: 3.5–7.2) on average, and then the right–left axis, measuring 3.7 ± 0.7 (range: 2.1–4.9) on average. A representative case illustrating the dipole artifact pattern seen on T1-weighted images and plots of artifacts' dimensions is presented in Fig. 2.

Interestingly, in addition to the main SI void artifact, a high-signal, mostly continuous, peripheral, rim-like artifact was noticed in various sequences. This was of special radiological significance on the post-contrast and subtracted T1-weighted images, in which, on several slices, a peripheral high-SI focus artifact appeared, mimicking a suspicious enhancement. Representative cases illustrating the typical rim and the "pseudo-enhancement" focus high-SI artifacts on T1-weighted images are presented in Figs. 3 and 4.

When comparing artifacts' dimensions on the various unenhanced MRI sequences, the sequence with the most prominent artifact, as measured on the axial plane, was DWI, measuring 8.9 ± 2.2 cm (range: 5.5–14.3) on average ($p < 0.001$) at the largest diameter, followed by fat-suppressed T2-weighted images, measuring 4.6 ± 0.8 cm (range: 3.2–6.4), and non-fat-suppressed T1-weighted images, measuring 4.3 ± 0.8 cm (range: 2.9–6.4). Artifacts on DWI were characterized by high SI, geometrical distortions, and associated ghosting artifacts in the phase-encoding axis. Representative cases illustrating the prominent artifacts on DW images ($n = 16$), acquired using either echo planar imaging (EPI) ($n = 13$) or the multiplexed sensitivity-encoding (MUSE) ($n = 3$) sequences, are presented in Fig. 5.

Finally, no significant difference was found between the artifacts' largest diameter on T1-weighted and T2-weighted images as compared between scans performed on 1.5 T ($n = 8$) vs. 3.0 T ($n = 11$) ($p = 0.41$–0.86), excluding cases

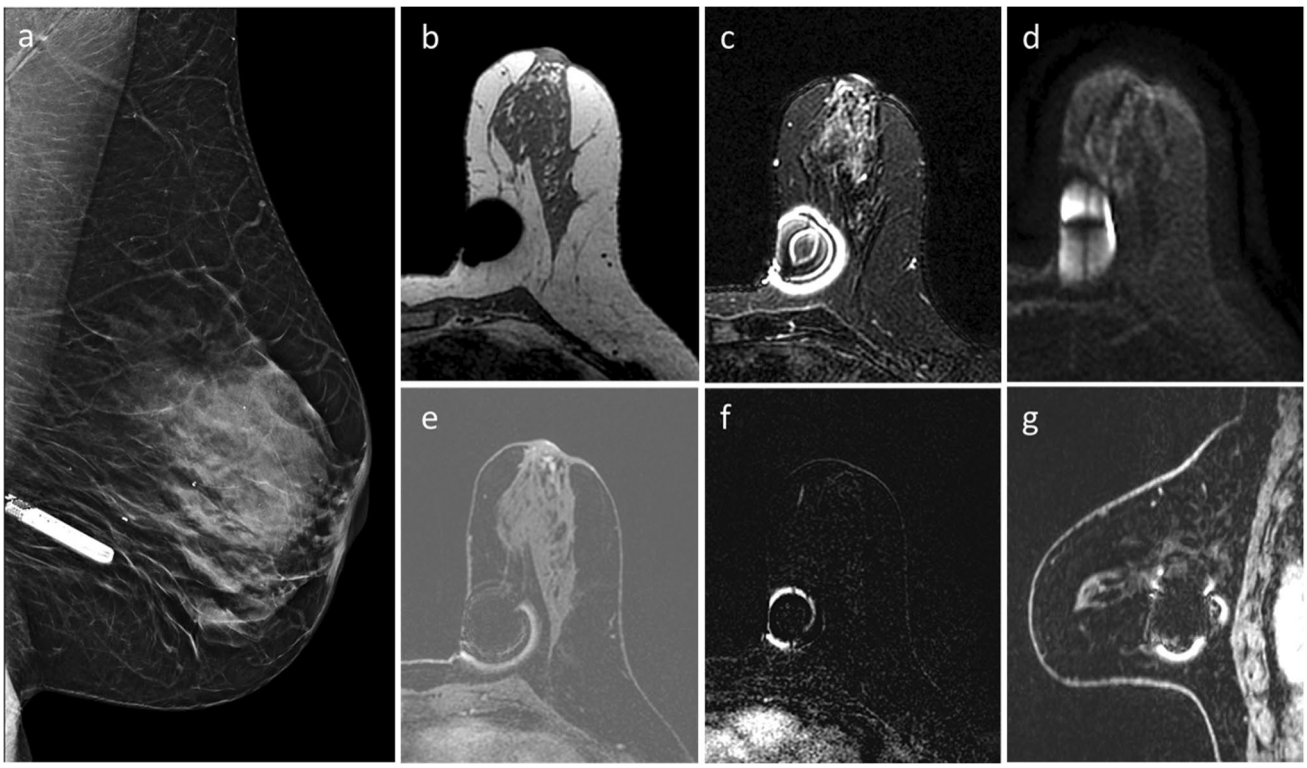

Fig. 1 Loop recorder artifact appearance on the various MRI sequences. Images of a representative 64-year-old patient with implantable loop recorder. Left breast mammographic medio-lateral oblique (MLO) view reference (**a**) highlights the relatively small dimensions of the device and its position at the lower-inner breast. Non-fat-suppressed pre-contrast T1-weighted image reveals signal void in the device bed (**b**). High signal void artifact is demonstrated on fat-suppressed T2-weighted image (**c**) and diffusion-weighted image (**d**), with associated geometrical distortions in the latter. Post-contrast axial (**e**), subtracted (**f**), and sagittal (**g**) T1-weighted images exhibit both central signal void and peripheral non-continuous "ring-like" artifacts. Interestingly, the dipole pattern of inhomogeneity induced by a cylindrical metal object is best visualized on the sagittal plane

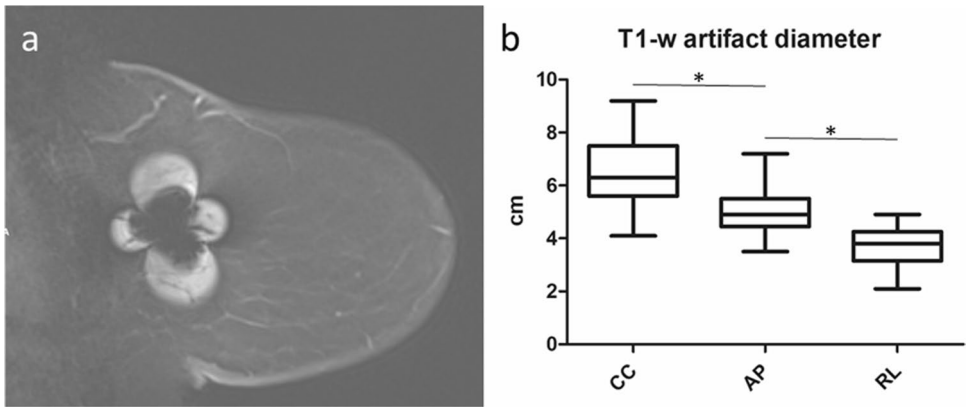

Fig. 2 Dipole artifact pattern on subtracted dynamic contrast-enhanced (DCE) T1-weighted images and artifact measurements in the three axes. Sagittal post-contrast T1-weighted image (**a**) of a representative 69-year-old patient with implantable loop recorder, exhibiting the typical dipole, four-leaf-clover-like artifact with central signal intensity (SI) void and four round high-SI artifacts, prominent on the cranio-caudal (CC) axis, and representing the interference of the implantable loop recorder with the magnetic field. Plots of box ((median ± interquartile range (IQR)) and whiskers (1.5 IQR) of the artifacts' measurements in the three orthogonal dimensions, confirming the largest dimension on CC axis, followed by the anterior–posterior (AP) axis, and the right–left (RL) axis (**b**)

performed at outside facilities ($n=14$), and sequential scans of the same patient ($n=7$).

Findings on MRI and MRI-guided biopsies

There were 23/40 (58.5%) negative MRI examinations. In 9/40 (22.5%) with known right ($n=5$) or left ($n=4$) breast cancer, the tumor was visualized with no additional suspicious findings. In 8/40 (20%), MRI showed suspicious findings. Eight MRI-guided biopsies were performed, resulting in four malignant findings (one contralateral and three additional ipsilateral to known cancers), and four benign findings. Of the six cases with left breast cancer, ipsilateral to the ILR, the tumor was distant from the artifact area and completely visible in five cases, and partially obscured by the artifact in one exam. A representative case demonstrating the utility of MRI-guided breast biopsy in the presence of ipsilateral ILR is presented in Fig. 6.

Discussion

Our initial experience performing breast MRI in the presence of ILR was successful; all diagnostic examinations and MRI-guided biopsies were performed without cancelations, no safety concerns arose, and, from a clinical standpoint, breast MRI provided additional diagnostic information with limited compromise.

Our results indicate that presence of an ILR among patients undergoing breast MRI is relatively uncommon and noted in < 0.1% of breast MRI studies. Nevertheless, the actual incidence might be higher, since our results rely on a specific keyword search, potentially excluding exams without "loop recorder" reported by the radiologist. Accordingly, a recent study on mammography utilization among patients with pacemaker reported that in up to 16% of cases the coexistence of pacemaker was not reported [17].

MRI in patients with therapeutic implantable cardiac devices, such as permanent pacemakers and defibrillators, is performed with caution and often requires pre-procedural guidance and at times periprocedural device reprogramming or the attendance of a cardiologist during the examination, as the risk of device malfunctioning could be hazardous [18]. On the other hand, MRI in patients with ILRs has been shown to be safe [10, 14, 15, 19–24] as an ILR is a diagnostic-only device; as such, the impact of MRI in patients with ILR is minimal, though infrequent alteration or elimination of stored ILR data as well as recorded artifacts has been reported. Consequently, the Heart Rhythm Society recommends that prior to MRI, an ILR should be interrogated and clinically pertinent stored data should be downloaded and subsequently cleared prior to the scan [7]. In accordance, per our institutional policy, patients are advised and encouraged to share this information with their cardiologist, prior to the scan; current ILRs also allow for remote transmission which can be performed at any time prior to MRI. The MRI imaging parameters for these devices should follow the conditions listed by the manufacturer. It should be noted that patients with implantable ILRs are monitored for arrhythmias or conduction system disease that may have led to cryptogenic stroke or syncope. Even though the latter conditions are highly unlikely to manifest during the short time of an MRI scan, it is important to monitor the patient throughout according to standard institutional policies.

Technical challenges associated with MRI near metals are relatively common in the orthopedic setting, in which

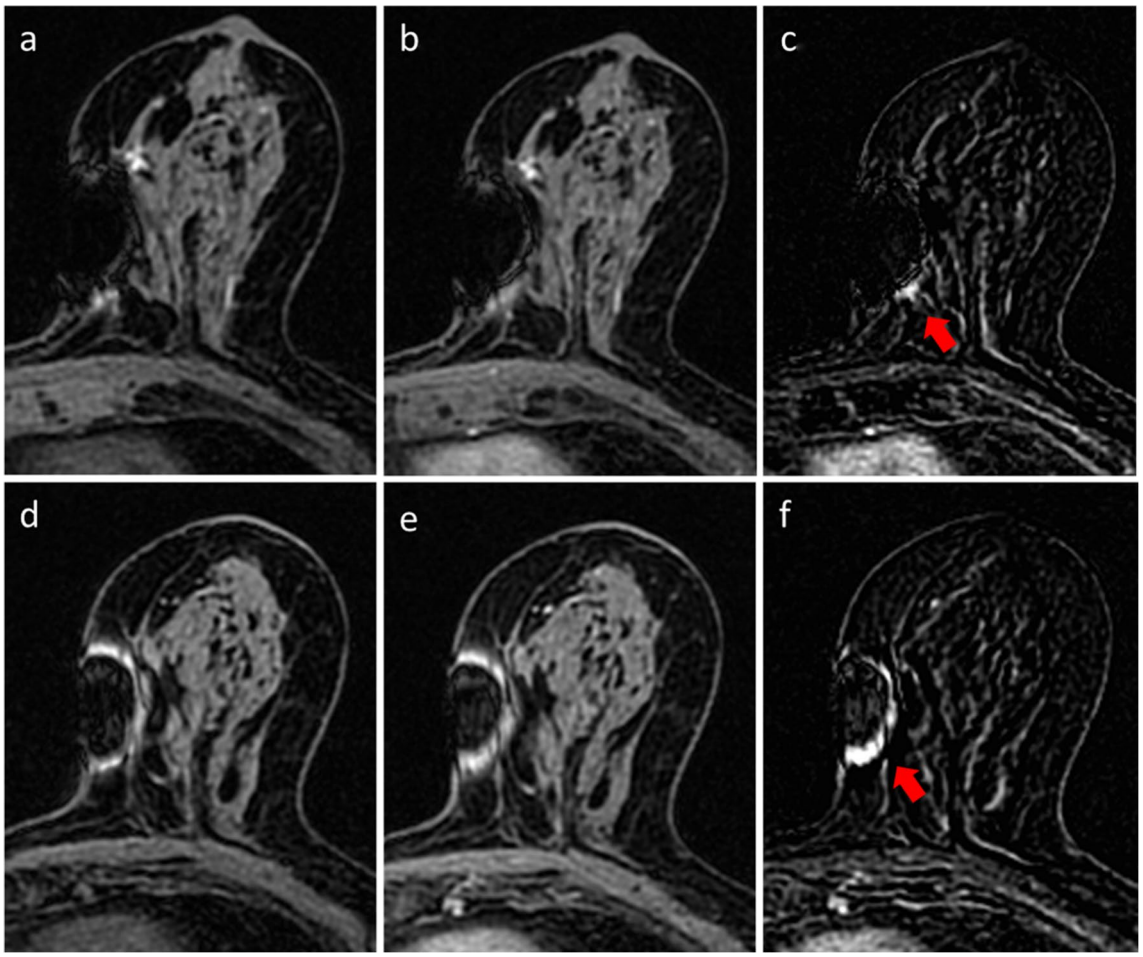

Fig. 3 "Pseudo-enhancement" artifact on subtracted dynamic contrast-enhanced (DCE) T1-weighted images. MRI of a 74-year-old patient with implantable loop recorder, screened due to personal history of breast cancer and extremely dense breasts. Two different slice locations are represented in each row. In the upper row, axial pre- (**a**) and post-contrast (**b**) T1-weighted images reveal central signal void artifact and additional similar but nonidentical high-signal foci. Subsequently, subtraction image (**c**) of the misregistered pre- and post-contrast images may show a "pseudo-enhancing" artifact, which could be misinterpreted as enhancing focus. In the second row, a more typical continuous, peripheral, ring-like high signal is noted on the pre (**d**), post (**e**), and subtracted (**f**) images, facilitating the diagnosis of loop recorder–induced artifact

numerous types of metals are frequently embedded and periprosthetic imaging is warranted [25]. In breast imaging, this scenario is less frequent. Still, several metallic devices may be encountered at the edge of the field of view, most commonly from proximal organs, including sternal wires, spinal or shoulder joint hardware, certain types of drug delivery ports, and cardiac devices [26]. Within the breast, susceptibility artifacts near surgical clips, tissue air interface [27], silicone implants [28], and biopsy markers are frequently encountered, though the latter are usually limited to a few millimeters [29] and provide an important role in guiding future interventions [30].

Our results highlight several technical drawbacks associated with ILRs implanted near the left breast. The ILR, as a spherical ferromagnetic material, acts as a dipole aligned to the magnetic field and leads to inhomogeneity of signal suppression, as well as enhancement of the local field (B0), resulting in a four-leaf clover pattern of low- and high-SI artifacts, respectively [31]. Accordingly, we encountered differences in the artifacts' dimensions, which were greatest on the CC axis, orthogonal to the ILR plane. The dipole pattern of artifacts was less destructive on the axial plane, which most breast MRI protocols rely on, exhibiting smaller artifact dimensions in parallel and anti-parallel to the device. However, ILR-associated artifacts may be more harmful for MRI-guided biopsies, which are executed in sagittal views [32].

Two forms of artifacts are associated with MRI containing metal devices. The first is related to signal loss in the area surrounding the device as a result of magnetic field changes, causing significant dephasing of the signal and signal loss [22]. Indeed, we encountered a signal

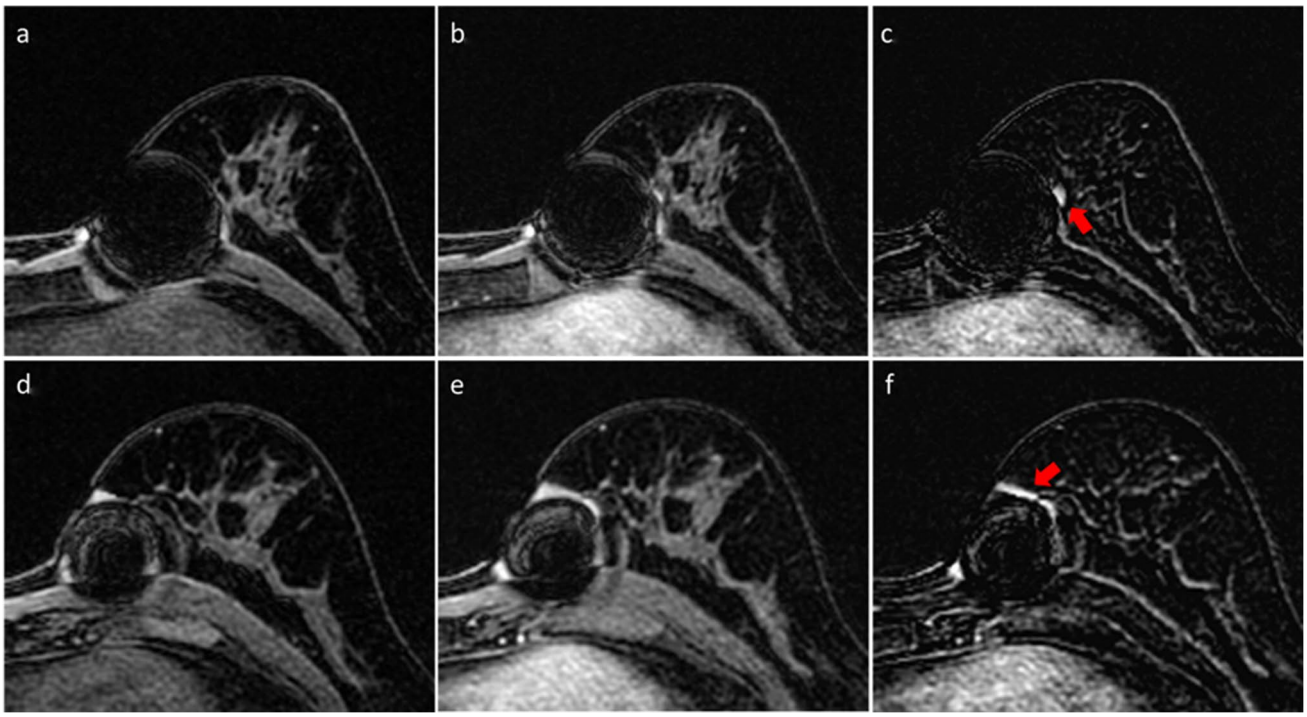

Fig. 4 "Pseudo-enhancement" artifact on subtracted dynamic contrast-enhanced (DCE) T1-weighted images. MRI of a 54-year-old patient with implantable loop recorder, screened due to family history of breast cancer. Two different slice locations are represented in each row. In the upper row, axial pre- (**a**) and post-contrast (**b**) images reveal central signal void artifact and additional similar but nonidentical high-signal foci, which result in a "pseudo-enhancing" artifact on the subtracted respective T1-weighted image (**c**). Further inferiorly, the ring-like high signal on the pre (**d**), post (**e**), and subtracted (**f**) images confirms the presence of a characteristic loop recorder–induced artifact

void in the ILR bed, which limited visualization in the partially obscured inner breast. The SI loss was mostly localized in the inner lower breast, though measurements varied between patients, probably due to differences in ILR position and size, which vary according to manufacturer (Medtronic Reveal LINQ (45 × 7 × 4 mm), Biotronik BioMonitor 2 (88 × 15 × 6 mm), Abbott Confirm Rx (49 × 9 × 3 mm)) [6], and dictate the artifact extent in the device bed. Nevertheless, from a diagnostic performance perspective, reduced sensitivity due to decreased visibility of this quadrant should be less likely, since this area of the breast is the least frequent location of breast cancers, accounting for only 7% of malignancies [33].

The second type of artifact is related to signal hyperintensity in DCE T1-weighted images. In the presence of metallic objects, the local magnetic field homogeneity is disturbed; in addition to signal loss, the signal can also accumulate in one region, resulting in pile-up artifact effects, whereby misregistered signal is shifted away from a position [34]. These regions exhibit increased SI, which may mimic suspicious contrast enhancement [21]. As shown in the related figures, these hyper-intensities usually exhibit continuous, peripheral, rim-like shapes, and therefore can be readily identified as artifacts. Yet, we also demonstrated how, on given slices, "pseudo-enhancing" foci may be displayed. This is a potential pitfall that radiologists should be aware of, highlighting the importance of scrolling through DCE-MRI slices to recognize the artifact pattern in sequential slices[35].

Our results also highlight the vulnerability of DWI for field inhomogeneity. Breast DWI has shown clinical promise [36], and attempts have been made to integrate this method into routine practice [37]. Typically, breast DWI is rapidly applied using EPI to avoid motion artifacts. However, EPI is highly sensitive to field variations, and tends to drastically underperform in the proximity of metal. Consequently, and in agreement with our results, it is well-established that DWI in general [38] and breast DWI in particular [39] are prone to susceptibility artifacts. In recent years, several alternative pulse sequences to diffusion-based EPI have been developed [40–43], but these have not been attempted near metals, whereas other advanced MRI techniques specifically designed for reducing metal-induced artifacts have yet to be studied for breast [44, 45], leaving this an area for future research.

From a clinical perspective, and despite the above-mentioned limitations, MRI examinations and procedures in women with ILR did provide added diagnostic

Fig. 5 Loop recorder–induced artifacts and geometrical distortions on diffusion-weighted images. Diffusion-weighted (DW) images of four different patients with implantable loop recorder, scanned with either echo planar imaging (EPI)–based (**a** and **c**) or multiplexed sensitivity-encoding (MUSE)–based (**b** and **d**) techniques. Interestingly, each features a different artifact appearance: EPI-DW images are characterized by vertical geometrical distortion artifact along the phase-encoding axis, whereas MUSE-DWI images exhibit horizontal ghosting artifact in the readout axis

value, to information obtained by conventional diagnostic workup with mammography and ultrasound. Nevertheless, despite the advantages, MRI visualization of the loop recorder area is more limited compared with mammography [4, 6], as could also be appreciated in Fig. 1. Therefore, the possibility of missed cancers adjacent to the ILR must be considered.

Limitations of this study include the small patient population and the fact that it is a single-institution study. Based on this cohort, we could not accurately quantitate the potential

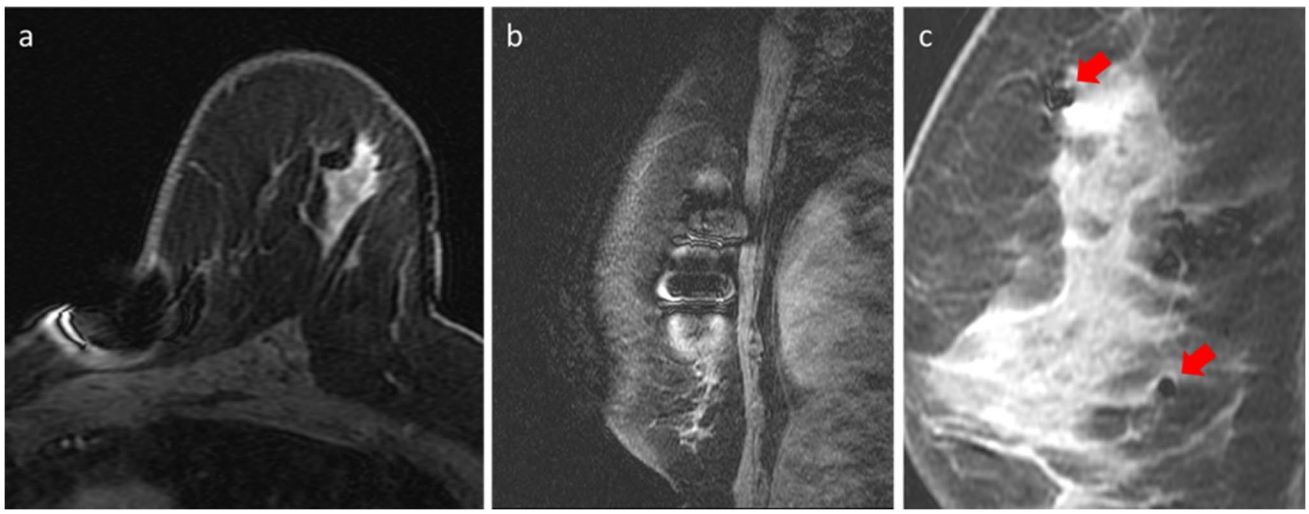

Fig. 6 MRI-guided breast biopsy in the presence of ipsilateral loop recorder. MRI of a 57-year-old patient with implantable loop recorder and newly diagnosed left breast invasive mucinous carcinoma, for whom MRI-guided biopsy was recommended and successfully performed at two sites. Axial post-contrast T1-weighted image (**a**) demonstrates the device artifact in the upper inner breast, as well as the non-mass enhancement in the upper outer breast with susceptibility artifact in its anterior extent, denoting site of biopsy. Sagittal images at medial (**b**) and lateral (**c**) positions respectively show the typical dipole artifact on the cranio-caudal (CC) plane and the two small susceptibility artifacts, corresponding with biopsies sites (arrows)

for false negative examinations. In addition, the inclusion of patients scanned on different scanners and protocols may add variability to the measurements performed. Finally, our safety analysis was limited to evaluation of patient- or device-related adverse effects, while assessment of ILR tracing artifacts or impact on stored data was beyond the scope of this study.

Conclusions

Our initial experience with breast MRI examinations and MRI-guided biopsies in patients with loop recorders shows that these procedures are feasible and safe. Despite associated artifacts that should be taken into consideration, breast MRI, when indicated, can provide added diagnostic value in this patient population.

Supplementary information The online version contains supplementary material available at https://doi.org/10.1007/s00330-023-10025-3.

Acknowledgements The authors thank Garon Scott for editing the manuscript.

Funding This work was supported in part through the NIH/NCI Cancer Center Support Grant P30 CA008748.

Declarations

Guarantor The scientific guarantor of this publication is Dr. Maxine Jochelson.

Conflict of interest Katja Pinker is a member of the *European Radiology* Scientific Editorial Board. She has not taken part in the review or selection process of this article. The authors of this manuscript declare no relationships with any companies whose products or services may be related to the subject matter of the article.

Statistics and biometry One of the authors has significant statistical expertise.

Informed consent Written informed consent was waived by the Institutional Review Board.

Ethical approval Institutional Review Board approval was obtained.

Study subjects or cohorts overlap No overlap.

Methodology
- Retrospective
- Observational
- Performed at one institution

References

1. Bisignani A, De Bonis S, Mancuso L et al (2018) Implantable loop recorder in clinical practice. J Arrhythmia. 35(1):25–32
2. Radovanović NN, Pavlović SU, Kirćanski B et al (2021) Diagnostic value of implantable loop recorders in patients with unexplained syncope or palpitations. Ann Noninvasive Electrocardiol. https://doi.org/10.1111/anec.12864
3. Solano A, Menozzi C, Maggi R et al (2004) Incidence, diagnostic yield and safety of the implantable loop-recorder to detect the mechanism of syncope in patients with and without structural heart disease. Eur Heart J. https://doi.org/10.1016/j.ehj.2004.05.013
4. Steinberger S, Margolies LR (2017) The implantable loop recorder and its mammographic appearance: a case based approach. Clin Imaging. https://doi.org/10.1016/j.clinimag.2017.01.006
5. Mayo RC, Leung J (2017) Novel wireless cardiac monitor located in the breast: imaging appearance and function. Breast J 23(5):599–601
6. Nia ES, Huang ML, Sun SX et al (2021) The mammographic appearance of the BioMonitor implantable loop recorder. Clin Imaging. https://doi.org/10.1016/j.clinimag.2020.11.051
7. Paap E, Witjes M, Van Landsveld-Verhoeven C et al (2016) Mammography in females with an implanted medical device: impact on image quality, pain and anxiety. Br J Radiol. https://doi.org/10.1259/bjr.20160142
8. Koch KM, Hargreaves BA, Pauly KB et al (2010) Magnetic resonance imaging near metal implants. J Magn Reson Imaging 32(4):773–87
9. Yang E, Suzuki M, Nazarian S, Halperin HR (2022) Magnetic resonance imaging safety in patients with cardiac implantable electronic devices. Trends Cardiovasc Med 32(7):440–447
10. Gimbel JR (2008) Magnetic resonance imaging of implantable cardiac rhythm devices at 3.0 tesla. Pacing Clin Electrophysiol. https://doi.org/10.1111/j.1540-8159.2008.01117.x
11. Hilbert S, Jahnke C, Loebe S et al (2018) Cardiovascular magnetic resonance imaging in patients with cardiac implantable electronic devices: a device-dependent imaging strategy for improved image quality. Eur Heart J Cardiovasc Imaging. https://doi.org/10.1093/ehjci/jex243
12. Reiter T, Weiss I, Weber OM, Bauer WR (2022) Signal voids of active cardiac implants at 3.0 T CMR. Sci Rep 12:1–11. https://doi.org/10.1038/s41598-022-09690-z
13. Vuorinen AM, Lehmonen L, Karvonen J et al (2022) Reducing cardiac implantable electronic device–induced artefacts in cardiac magnetic resonance imaging. Eur Radiol. https://doi.org/10.1007/s00330-022-09059-w
14. Nazarian S, Beinart R, Halperin HR (2013) Magnetic resonance imaging and implantable devices. Circ Arrhythmia Electrophysiol. https://doi.org/10.1161/CIRCEP.113.000116
15. van der Graaf AWM, Bhagirath P, Götte MJW (2014) MRI and cardiac implantable electronic devices; current status and required safety conditions. Netherlands Hear J 22(6):269–76
16. Daimiel Naranjo I, Lo Gullo R, Saccarelli C et al (2021) Diagnostic value of diffusion-weighted imaging with synthetic b-values in breast tumors: comparison with dynamic contrast-enhanced and multiparametric MRI. Eur Radiol. https://doi.org/10.1007/s00330-020-07094-z
17. Nissan N, Moss Massasa EE, Bauer E et al (2023) Pacemaker in patients undergoing mammography : a limitation for breast cancer diagnosis ? J Med Imaging Radiat Oncol 8–1. https://doi.org/10.1111/1754-9485.13524
18. Bovenschulte H, Schlüter-Brust K, Liebig T et al (2012) MRI in patients with pacemakers: overview and procedural management. Dtsch Arztebl Int 109(15):270–275
19. Blaschke F, Lacour P, Walter T et al (2016) Cardiovascular magnetic resonance imaging in patients with an implantable loop recorder. Ann Noninvasive Electrocardiol. https://doi.org/10.1111/anec.12333
20. Gimbel JR, Zarghami J, Machado C, Wilkoff BL (2005) Safe scanning, but frequent artifacts mimicking bradycardia and tachycardia during magnetic resonance imaging (MRI) in patients with an implantable loop recorder (ILR). Ann Noninvasive Electrocardiol. https://doi.org/10.1111/j.1542-474X.2005.00056.x

21. Runge M, Ibrahim ESH, Bogun F et al (2019) Metal artifact reduction in cardiovascular MRI for accurate myocardial scar assessment in patients with cardiac implantable electronic devices. AJR Am J Roentgenol 213(3):555–561
22. Stojanovska J, Runge M, Mahani MG et al (2020) Cardiac MRI for patients with cardiac implantable electronic devices. AJR Am J Roentgenol. https://doi.org/10.2214/AJR.19.21883
23. Nazarian S, Halperin HR (2009) How to perform magnetic resonance imaging on patients with implantable cardiac arrhythmia devices. Hear Rhythm. https://doi.org/10.1016/j.hrthm.2008.10.021
24. Wong JA, Yee R, Gula LJ et al (2008) Feasibility of magnetic resonance imaging in patients with an implantable loop recorder. Pacing Clin Electrophysiol. https://doi.org/10.1111/j.1540-8159.2008.00994.x
25. Galley J, Sutter R, Stern C, et al (2020) Diagnosis of periprosthetic hip joint infection using MRI with metal artifact reduction at 1.5 T. Radiology. https://doi.org/10.1148/radiol.2020191901
26. Hargreaves BA, Daniel BL (2012) Metals in MR-mammography: how to deal with it? Eur J Radiol. https://doi.org/10.1016/S0720-048X(12)70021-9
27. Borde T, Wu M, Ruschke S et al (2022) Assessing breast density using the chemical-shift encoding-based proton density fat fraction in 3-T MRI. Eur Radiol. https://doi.org/10.1007/s00330-022-09341-x
28. Solomon E, Nissan N, Schmidt R et al (2016) Removing silicone artifacts in diffusion-weighted breast MRI by means of shift-resolved spatiotemporally encoding. Magn Reson Med. https://doi.org/10.1002/mrm.25757
29. Genson CC, Blane CE, Helvie MA et al (2007) Effects on breast MRI of artifacts caused by metallic tissue marker clips. AJR Am J Roentgenol. https://doi.org/10.2214/AJR.05.1254
30. Eskreis-Winkler S, Simon K, Reichman M et al (2020) Dipole modeling of multispectral signal for detecting metallic biopsy markers during MRI-guided breast biopsy: a pilot study. Magn Reson Med. https://doi.org/10.1002/mrm.28017
31. Lee EM, Ibrahim ESH, Bs ND et al (2021) Improving MR image quality in patients with metallic implants. Radiographics. https://doi.org/10.1148/rg.2021200092
32. Lambert J, Steelandt T, Heywang-Köbrunner SH et al (2021) Long-term MRI-guided vacuum-assisted breast biopsy results of 600 single-center procedures. Eur Radiol. https://doi.org/10.1007/s00330-020-07392-6
33. Sarp S, Fioretta G, Verkooijen HM et al (2007) Tumor location of the lower-inner quadrant is associated with an impaired survival for women with early-stage breast cancer. Ann Surg Oncol. https://doi.org/10.1245/s10434-006-9231-5
34. Hargreaves BA, Worters PW, Pauly KB et al (2011) Metal-induced artifacts in MRI. AJR Am J Roentgenol. https://doi.org/10.2214/AJR.11.7364
35. Kapsner LA, Ohlmeyer S, Folle L et al (2022) Automated artifact detection in abbreviated dynamic contrast-enhanced (DCE) MRI-derived maximum intensity projections (MIPs) of the breast. Eur Radiol 32:5997–6007. https://doi.org/10.1007/s00330-022-08626-5
36. Partridge SC, Nissan N, Rahbar H et al (2017) Diffusion-weighted breast MRI: clinical applications and emerging techniques. J Magn Reson Imaging 45(2):337–355
37. Lo Gullo R, Sevilimedu V, Baltzer P et al (2022) A survey by the European Society of Breast Imaging on the implementation of breast diffusion-weighted imaging in clinical practice. Eur Radiol 32:6588–6597. https://doi.org/10.1007/s00330-022-08833-0
38. Le Bihan D, Poupon C, Amadon A (2006) Lethimonnier F (2006) Artifacts and pitfalls in diffusion MRI. J Magn Reson Imaging. 24(3):478–88
39. Furman-Haran E, Eyal E, Shapiro-Feinberg M et al (2012) Advantages and drawbacks of breast DTI. Eur J Radiol. https://doi.org/10.1016/S0720-048X(12)70017-7
40. Granlund KL, Staroswiecki E, Alley MT et al (2014) High-resolution, three-dimensional diffusion-weighted breast imaging using DESS. Magn Reson Imaging. https://doi.org/10.1016/j.mri.2013.12.014
41. Solomon E, Nissan N, Furman-Haran E et al (2015) Overcoming limitations in diffusion-weighted MRI of breast by spatio-temporal encoding. Magn Reson Med. https://doi.org/10.1002/mrm.25344
42. Solomon E, Liberman G, Nissan N et al (2020) Diffusion-weighted breast MRI of malignancies with submillimeter resolution and immunity to artifacts by spatiotemporal encoding at 3T. Magn Reson Med. https://doi.org/10.1002/mrm.28213
43. Sanderink WBG, Teuwen J, Appelman L et al (2021) Comparison of simultaneous multi-slice single-shot DWI to readout-segmented DWI for evaluation of breast lesions at 3T MRI. Eur J Radiol. https://doi.org/10.1016/j.ejrad.2021.109626
44. Lee PK, Yoon D, Sandberg JK et al (2022) Volumetric and multispectral DWI near metallic implants using a non-linear phase Carr-Purcell-Meiboom-Gill diffusion preparation. Magn Reson Med. https://doi.org/10.1002/mrm.29153
45. Koch KM, Bhave S, Gaddipati A et al (2018) Multispectral diffusion-weighted imaging near metal implants. Magn Reson Med. https://doi.org/10.1002/mrm.26737